Journal of
Earth Science & Climatic Change

Nusara et al., J Earth Sci Clim Change 2017, 8:1
DOI: 10.4172/2157-7617.1000384

Research Article Open Access

Petrology and Alteration of Calcium Sulphate Deposits in Late Paleozoic Rocks of Wang Saphung Area, Loei Province, Thailand

Nusara S[1]*, Punya C[2], Sarunya P[3] and Ken-Ichiro H[1]

[1]*Graduate School of Life and Environmental Sciences, University of Tsukuba, Japan*
[2]*Department of Geology, Faculty of Science, Chulalongkorn University, Bangkok, 10330, Thailand*
[3]*Department of Geotechnology, Faculty of Technology, Khon Kaen University, Khon Kaen, 40002, Thailand*

Abstract

The gypsum-anhydrite deposit in Loei-Wang Saphung (LWS) area of northeastern Thailand is a small evaporite sediment deposit with up to 50 m thick gypsum-anhydrite beds. The evaporite deposits are overlain by cross-laminated and fine-grained siliciclastic and carbonate rocks of the Carboniferous to Permian ages. This paper documents some characteristics of the deposits, including lithologies, textures, and structures of gypsum-anhydrite and associated rocks, based on the stratigraphic core logging of boreholes and lithofacies analysis of selected samples.

Morphological and textural mineralogical relationships reveal 10 textures of the evaporite formation viz. alabastrine gypsum, satin spar gypsum, selenite gypsum, gypsarenite, porphyroblastic gypsum, fine lenticular gypsum, crystalloblastic or blocky anhydrite, prismatic anhydrite, epigenetic anhydrite, and felty epigenetic anhydrite. The results also indicate that the LWS sulfate deposit has passed through at least 4 evolutionary alterations; (1) original precipitation as gypsum deposit, (2) gypsum-to-anhydrite transformation resulting from burial diagenesis in response to basinal subsidence, (3) rehydration of anhydrite-to-gypsum, indicated by distorted gypsum rocks, resulting from the increase of volume due to the rehydration from anhydrite to gypsum, and recrystallization of anhydrite and/or primary gypsum to secondary gypsum (4) uplift and re-expose of gypsum, indicated by the karstification and dissolution cavities and gypsarenite veins. The gypsum-anhydrite beds with associated carbonate and mud rocks suggest that these sedimentary sequences form in a subaqueous, probably shallow marine marginal setting during Late Carboniferous.

Keywords: Diagenesis; Gypsum-anhydrite deposits; Loei-Wang Saphung (LWS); Recrystallization; Rehydration

Introduction

Ancient evaporate including sulphates and rock salts are economically important not only as major sources for salt (such as halite and gypsum) and metal (such as Cu, Zn, and Ag minerals) but also as indications for structural trap of petroleum [1]. Thailand is one of the world leading producers of many non-metals including gypsum [2]. The identified resources of these minerals/rocks are being produced for domestic consumption and export [3]. According to DMR (1977), the evaporite/sulphate deposits are abundant in many parts of Thailand [4]. They can be grouped into 3 categories based upon their lithology and age association (Figure 1), including 1) deposits associated with Pre-Mesozoic rocks, 2) deposits associated with Mesozoic rocks, and 3) deposits associated with Post-Mesozoic rocks.

The Pre-Mesozoic evaporite deposits (gypsum/anhydrite) are located in Pichit-Nakhon Sawan area (central Thailand), Nakhon Sri Thamarat-Surat Thani area (southern Thailand), and Loei-Wang Saphung area (northeastern Thailand). The Mesozoic evaporite deposits (potash and rock salts) are much less widespread. They are restricted to the Khorat Plateau (Basin) which extends northward to Vientiane Basin in Lao PDR. The last deposit type is relatively uncommon and is frequently associated with the Neogene coal deposits. Among these, the Mae Moh coal deposits (northern Thailand) is the most economically essential.

Evaporites, particularly gypsums, have been exploited from the first and second types. According to the USGS [3], approximately 8.5 million to 10 million metric tons of gypsum have been mined annually. The gypsum deposits in Loei-Wang Saphung (LWS) area is estimated to be larger than 35 million tons from geophysical survey and drilling explorations [5,6]. However, little is known on the evaporite/sulphate deposits in Thailand. In the past, few researches that have been done so far, describe the lithology and some geochemistry of the deposits such as Pisutha-Arnond and El Tabahk and Utha-Aroon [7,8].This paper is therefore the first to document the presence of the sulphate deposit in the LWS area of northeastern Thailand by providing geological mapping, macroscopic and microscopic drilled core data analyses, and stratigraphic correlation. It is therefore our aim to pursue further detailed study on the gypsum/anhydrite deposits in this area. It is important to determine the location, geometry, and size of the deposits with respect to the geology of the study area. More detailed studies on geology, sedimentology, petrography, and paleontology of the deposits themselves as well as the detailed geologic controls and tectonic setting of the adjacent areas governing their transformation are needed to understand their geological depositional settings and diagenetic alteration history.

Geological Setting

Tectonics setting

The Loei and Petchabun fold belts were formed in response to convergent tectonics of the Shan-Thai and the Indochina terranes during closure of the Paleo-Tethys ocean by the end of Permian to early Triassic

***Corresponding author:** Nusara S, Graduate School of Life and Environmental Sciences, University of Tsukuba, Japan, Tel: 6643362125; E-mail: nussan@kku.ac.th

Received December 22, 2016; **Accepted** January 23, 2017; **Published** January 30, 2017

Citation: Nusara S, Punya C, Sarunya P, Ken-Ichiro H (2017) Petrology and Alteration of Calcium Sulphate Deposits in Late Paleozoic Rocks of Wang Saphung Area, Loei Province, Thailand. J Earth Sci Clim Change 8: 384. doi: 10.4172/2157-7617.1000384

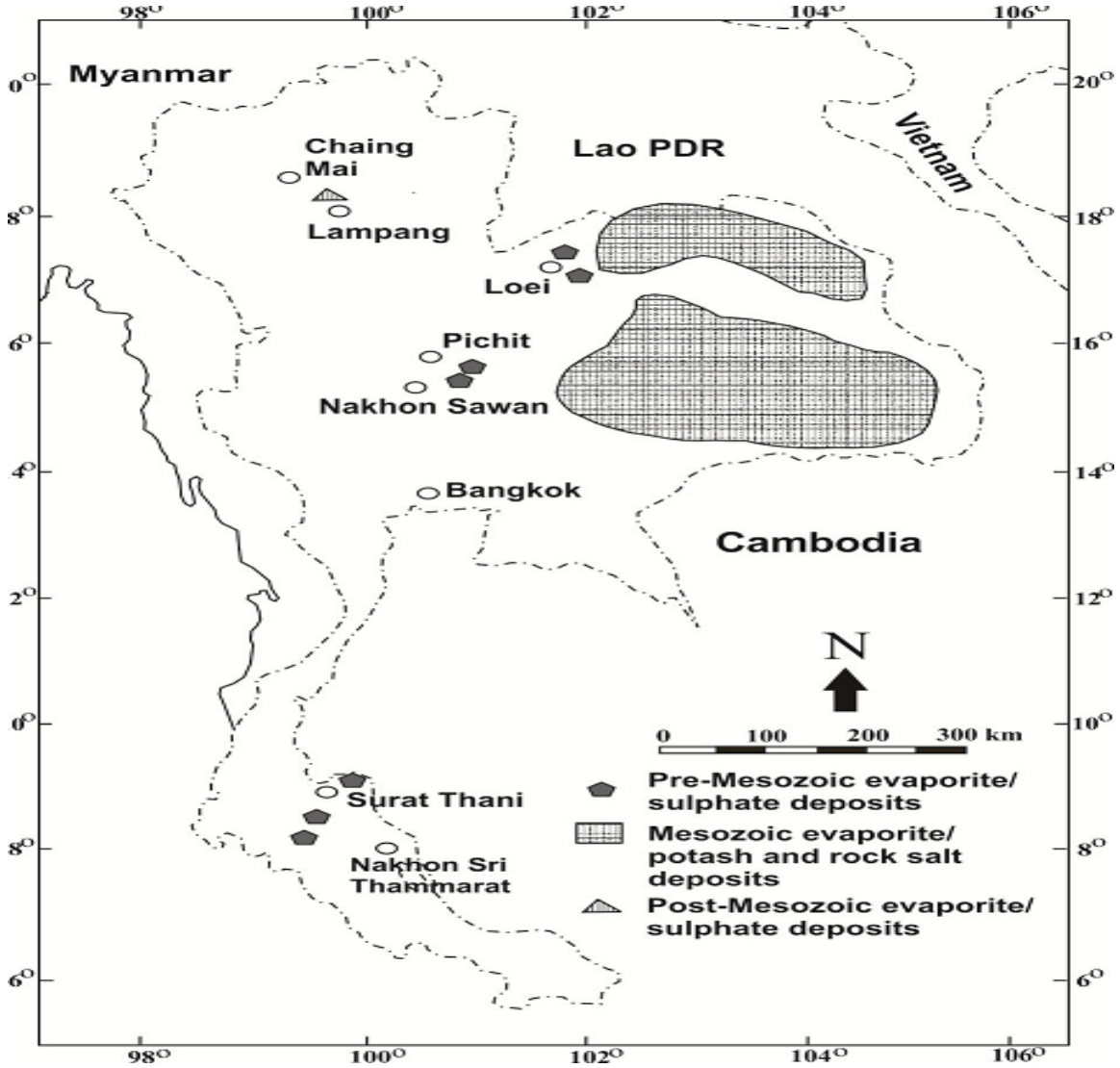

Figure 1: Map of Thailand showing locations of evaporite/sulphate deposits (modified after DMR in 1977 and Tabahk et al. in 1999).

[9-11]. These two belts trend roughly in the north-south direction and are exposed extensively in northeastern and central Thailand. The suture between the Shan-Thai and Indochina plates is marked by the Nan-Uttaradit Suture Zone and is characterized by an ophiolite belt [12-14]. Tectonic movements have resulted in the following features [8]: (1) compressional events during early Carboniferous Variscan Orogeny creating tight fold structures of pre-Permian strata; (2) back arc rifting during the Carboniferous and development of an extensive platform and basin; (3) late Permian/early Triassic Indosinian orogeny, interaction of the Indochina and the Shan-Thai terranes, and the closure of Paleo-Tethys ocean; (4) Triassic sag, development of foreland basin setting and deposition of the non-marine sediments of the Khorat Group covering the Permian platform in northeastern Thailand; and (5) early Tertiary compression and uplift of the Khorat Plateau.

Stratigraphy

The Loei area, where the LWS study area is located, is near the northwestern edge of the Khorat Plateau (Indochina terrane) [12,15]. The oldest rocks are low-grade meta-sedimentary rocks of Devonian age cropping out in the eastern part of the Loei area (Figure 2). The rocks are alternated with volcanic clastic rocks and overlain by the more widespread Carboniferous marine sedimentary rocks in the middle part. The Devonian strata are in contact with the overlying rocks by thrust fault [16]. The youngest sedimentary rocks are Permian marine strata, continental Mesozoic rocks (the Mesozoic Khorat Group), and recent sediments. The names and stratigraphic relationships of the rocks in Loei and adjacent area are shown in Figure 2.

Igneous rocks in Loei area are plutonic rocks consisting of granite, granodiorite, diorite, and hornblendite of Late Paleozoic to Early Mesozoic age and are spatially associated with volcanic rocks. The volcanic rocks are predominantly rhyolite, andesite, and dacite with a small amount of basalt which are distributed in three nearly north-south trending belts along the eastern, western, and central parts of the Loei area. Based on their field relation and geochronological data, volcanic rocks in Loei area are Middle Devonian-Early Carboniferous and Permo-Triassic age [17] studied the intrusion associated with the Cu-Au skarn formation near the Wang Saphung area, the intrusions (mainly diorite/granodiorite) are emplaced in the Carboniferous sedimentary rocks (Wang Saphung Formation). The U-Pb zircon and

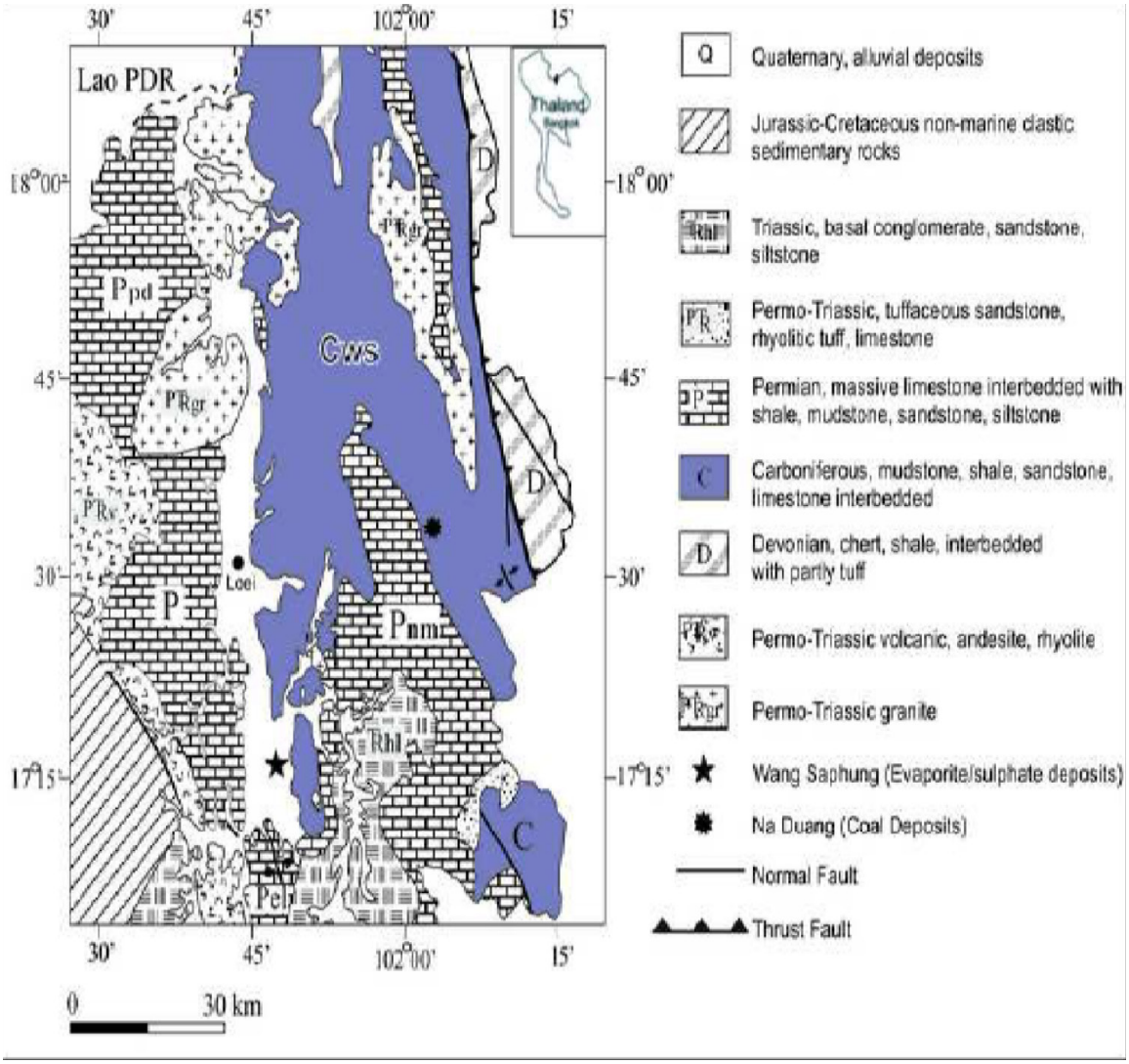

Figure 2: Simplified geological map of the Loei area, north-eastern Thailand, showing the location of the study area (modified after; DMR in 2010).

laser ablation Ar-Ar dating of biotite of the intrusions yields a Middle Triassic age 248–242 Ma. However, the intrusions also display younger feldspar $^{40}Ar/^{39}Ar$ age (*ca.* 164 ± 0.6 Ma) [18].

The study area lies in a narrow valley of Loei River in Wang Saphung District about 20 km south of Loei Province which is a part of a graben structure running roughly in the north–south direction. Much of the river valley is covered with semi-consolidated and recent alluvial sediments [6]. The valley is bounded on both sides by the north–south trending Late Paleozoic rocks which are well-exposed along the mountains [5]. According to the geological map by DMR [19], the eastern side of the exploration site is bounded by the Carboniferous rocks which are mapped as the Wang Saphung Formation (Cws). Farther east and south is the massive limestone of Pnm - Nam Maholan Formation (Early Permian). West and southwest of the exploration area (across the Loei River) is the thin bedded Pel-E-Lert Formation (Middle Permian). The nearest igneous outcrop inferred to be the Permo-Triassic volcanic rocks (rhyolite, andesite, and dacite) and located to the east of the exploration area belongs to the Cws Formation. The stratigraphic subdivisions of Carboniferous and Permian facies distribution in Loei area has been studied and named after the place of the type sections as shown in Figure 3.

The outcrops of the LWS gypsum deposits are found at shallow depth (2-3 meters below surface) particularly near Non Sawang temple. One outcrop was discovered in a laterite pit during the investigation in 1997 (Figure 4A), the other outcrop was discovered about 2 km east of Non Sawang Temple in a small pond (Figure 4B). The gypsum in the outcrop has a sugary texture (alabaster). Gypsum in both localities are present below unconsolidated alluvial sediments.

Facies Description and Interpretation

Stratigraphy

About 30 drilled holes with a total length of 1,799 meters have been investigated for evaporite (sulphate) deposits in the LWS area. All drilled holes are in terrace deposits, except that of No. 28 which is situated in alluvial deposits (Figure 5). From the results of lithostratigraphic and lithofacies analyses, 3 major pre-Cenozoic sedimentary rocks have been identified including carbonates, fine-grained clastic rocks, and evaporite (sulphate) facies.

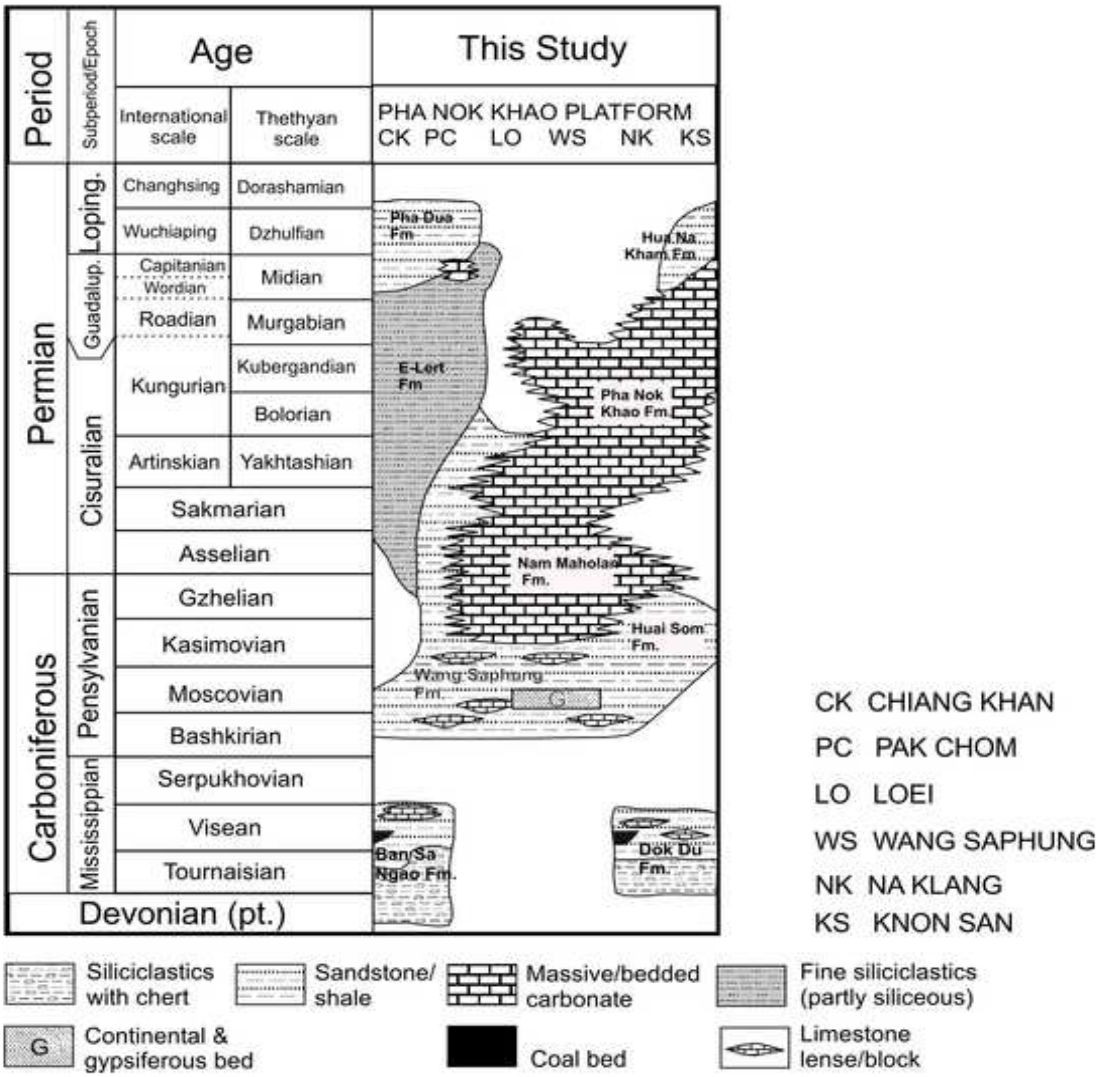

Figure 3: Carboniferous and Permian facies distribution and resulting stratigraphic subdivisions of the study area (modified after Ueno and Chareonthitirat in 2011).

Figure 4: Outcrops of shallow gypsum; (A) a gypsum boulder discovered in a laterite pit behind Non Sawang temple during 1997 (Kuttikul et al. in 1997); and (B) alabaster gypsum from an outcrop to the east of Non Sawang temple.

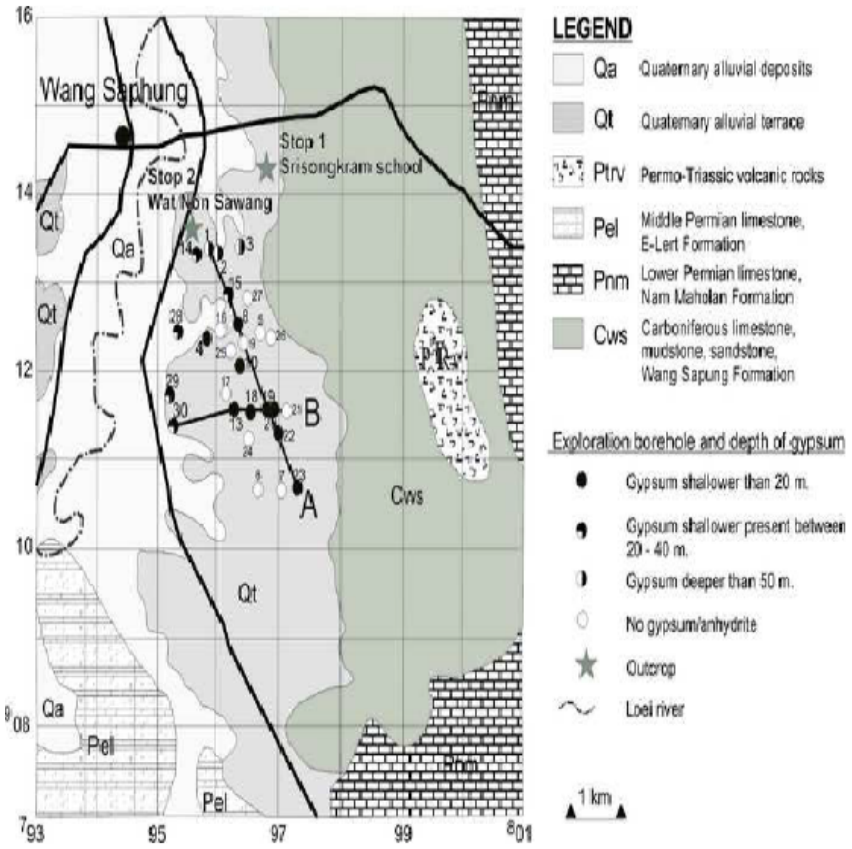

Figure 5: Geological map of the Loei-Wang Saphung (LWS) area showing the locations of boreholes and depth to top horizon of gypsum (modified from Kuttikul et al. in 1997).

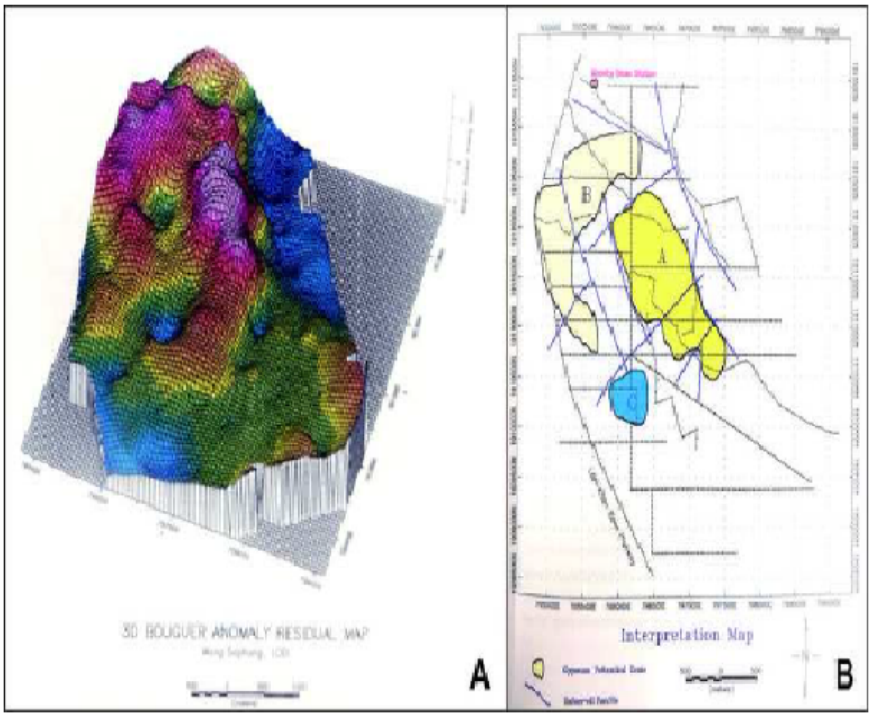

Figure 6: Schematic sulphate deposits of LWS area from a gravity survey by Kuttikul et al. in 1997; (A) 3D interpretation of an anomaly residual map; and (B) Interpretation map showing 3 highly potential gypsum areas with inferred faults in NNW-SSE and NE-SW directions.

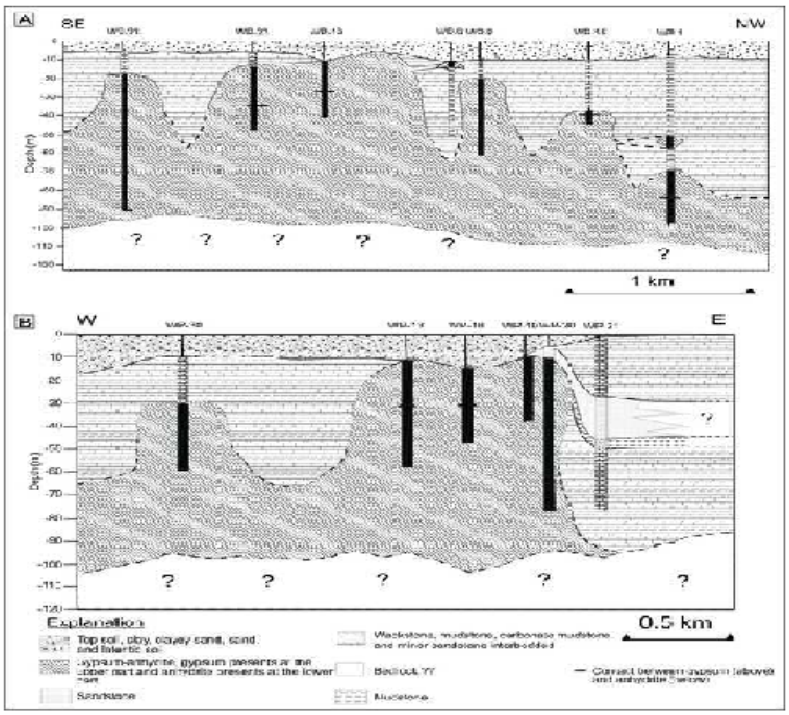

Figure 7: Schematic profile of sulphate deposits along (A) NW-SE and (B) E-W of the Wang Saphung area, showing the karst topography of the sulphate deposits.

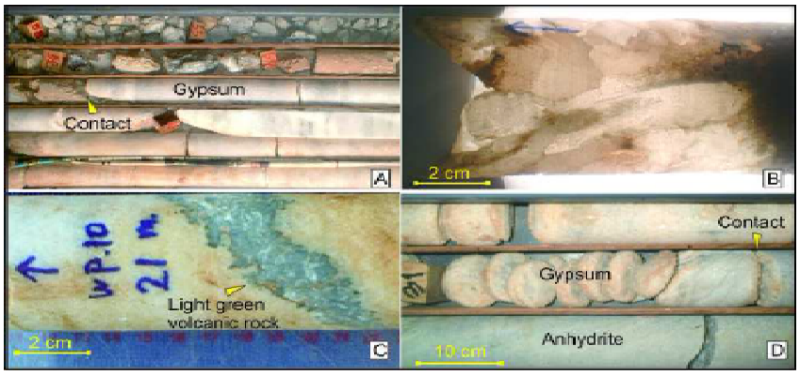

Figure 8: (A) Breccia clast above gypsum bed; (B) Large selenite gypsum; (C) Light green volcanic rock cross-cut in gypsum; and (D) Contact between gypsum-anhydrite.

The thickness of Quaternary sediments and top soils range from 2 to 10 meters. These unconsolidated sediments have a maximum thickness in the east where the holes encounter colluvial deposits. Beneath the top soil and Quaternary sediments, the predominant facies comprise of carbonate strata with a thickness varying from 1 to 40 meters. These carbonate facies beds consist largely of light to dark grey laminated mudstone, wackstone and packstone, algal boundstone, and fenestral carbonate mudstone based on Dunham (1962)'s classification [20]. The most common carbonate rocks found in the boreholes are the carbonate mudstone and wackstone. Sedimentary structures found in these lithofacies are lamination, bird's eye structure, bioturbation, stylolites, and fracture. Most of the fractures are filled by calcite. Pyrite is also abundant in these carbonate beds with some other heavy minerals.

These carbonate lithofacies are sometimes interbedded with fine-grained siliciclastic rocks. The latter range is in thickness from 1 to 20 meters. The light to yellowish brown, well-bedded to laminated sandstone with a thickness of 1 to 20 meters seem to be less common than the dark grey to black mudstone/siltstone with a thickness of 2 to 30 meters.

Few fossils have been reported from the cores and from surface mapping near the exploration area (Stop 1 in Figure 5). The fossils from the outcrop (Stop 1) are brachiopods, crinoids, and fusulinids. The fusulinid from the outcrop was identified to be *Beedeina sp.* of the Moscovian (Middle Carboniferous) age, while the fossils in the borehole studied by Fontain yield the age of Late Moscovian to late Permian [21]. However, the gypsum-anhydrite does not show any clear stratigraphic relationship with the carbonate rocks nor siliciclastic rocks in the exploration wells.

Although, not exposed anywhere in the exploration drilling area, felsic to intermediate volcanic rocks have been discovered at depth in the boreholes. A few occur as small dikes (up to 10 cm thick) cross-

cutting the gypsum beds. The rhyolite from drilled hole WP10 at 11.5 meters was sent for geochronological analysis. The dating of plagioclase feldspar yields an age of 140.8±3.1 Ma which is younger than the intrusion age reported by previous works.

Evaporite geometry of the sulphate deposits and their lithological contacts

The gypsum presents a karst-type relief like that developed in limestone. The solution of gypsum produces landforms that are different in size and characteristics. Most forms are the result of space and time distribution of the chemical solution in relation to different hydrodynamic and hydrological processes. Geological, geomorphological, climatic, and biological factors control these processes. The geometry of the evaporite bodies are shown in Figure 6, which is inferred from a gravity survey interpretation, and Figure 7, which is inferred from core log interpretation. Figure 6A shows a 3D gravity model based on Bougeur anomaly residual data interpretation by Kuttikul which presents 3 discontinuous high potential zones of sulphate minerals [6]. They interpreted that the discontinuity of the sulphate bodies are caused by a structural control. There are at least 2 sets of faults, NNW-SSE and NE-SW directions partially separating the deposits into blocks (Figure 6B). They proposed that the evidence supporting this interpretation is the abrupt change of the sulphate body within the area. For example, drill holes WP8 and WP9, which are located only about 100 meters apart, reveal gypsum at very different depths (Figure 7A). In WP8, the gypsum is found at 19 meters, while in WP9, the presence of gypsum is deeper at 34 meters. A similar discrepancy is also found between drill holes WP20 and WP21 (Figure 7B).

In this research, the geometry of sulphate bodies are interpreted by correlation of core logs (Figures 7A and 7B). We interpret that the abrupt change of the depth of sulphate may be caused by weathering and erosion processes. Karst topography or the karstification of sulphate is a result of the solution process under different hydrodynamic behaviors of gypsum. Supporting evidence of weathering and erosion are the breccia clast of the associated rocks at the contact top of the gypsum body (Figure 8A). The rocks display dissolution features, karstification, and cavities at depth. Some of the cavities contain large, elongated, saber-like gypsum crystals. Each crystal can be up to 3 cm long (Figure 8B). The gypsum body may have been uplifted and exposed to the surface and been through weathering and erosion before the deposition of recent fluvial sediments.

Lithological contact of the LWS sulphate deposits with other rocks are recognized in almost all drilled holes. They can be divided into 4 types including; 1) those with carbonate rocks, 2) those with siliciclastic rocks, 3) those with minor intrusive, and 4) those with slight alteration to anhydrite.

The contact with the carbonate rocks are present throughout the holes in various positions such as with carbonate rocks lying above, and interbedded or intercalated with gypsum and other rocks. Uncommonly, some contacts are found between the gypsum-anhydrite at the end of the boreholes. In some places, cores of carbonate rocks are broken and some are interpreted to be the result of karstification.

The contact with the siliciclastic rocks are occasionally found in some boreholes as interbeds with both carbonate rocks and gypsum. The siliciclastic beds compose mainly of intercalated mudstone and sandstone, some beds are sand dominant and some beds are mud dominant.

The third type of contact is occasionally found in some drilled holes such as WP11, WP15, and WP29 at depth. In this area, volcanic rocks are exposed in the eastern part of the investigation area and are quite common in the surrounding area. These are identified as Permo-Triassic age [17,22]. Igneous rocks in the boreholes are andesitic to rhyolitic dikes with a maximum thickness of 40 cm. Minor intrusions in the drilled cores show thin andesitic and rhyolitic rocks cross-cutting the gypsum layers (Figure 8C).

The fourth type of contact can be clearly observed in almost all drilled holes (Figure 8D). The gypsums gradually change to anhydrite at depth 25 – 85 meters. This can be observed by the lithology change from loose sugary texture of gypsum to dense and hard texture of anhydrite.

Petrology and alteration of calcium sulphates

The LWS calcium sulphates deposits consists of 5 main lithologies including carbonate rocks, siliciclastic rocks, sulphate rocks, breccia-conglomerate, and volcanic rocks. The sulphate rocks occur at depth, ranging from less than 10 meters to more than 50 meters under the ground surface, as a small evaporite body. The deposits comprise of gypsum-anhydrite beds interbedded with carbonate and siliciclastic rocks and are covered by unconsolidated Quaternary sediments.

Gypsum-anhydrite: The gypsum-anhydrite facies are present as laminae, which are 0.5 to 2.0 cm thick, of milky white gypsum-anhydrite separated by thin (<0.25 mm), dark gray to dark gray-brown, even to wavy and discontinuous thin seams and clasts of dolomitic limestone, carbonate mudstone, and mudstone. The character of the bedding varies from even and nearly flat to wavy with small amplitude folds to discontinuous (Figures 9A and 9B). The sulphate deposits are accompanied by carbonate rocks, silicic-clastic rocks, and breccia-conglomerate. No clear nodular anhydrites have been observed in this study. Generally, most of the gypsum have a white sacharoidal appearance and commonly show knotty structure or enterolithic fold (snaky gypsum) due to disordered swelling deformation. They change to anhydrite with even carbonate and clay lamination at depth.

The evaporite facies from the LWS area were characterized petrographically through the analysis of 66 thin sections. Based on morphology and crystal relationships, 10 phases of evaporite formation were recognized, which include: 1. alabastrine gypsum, 2. satin spar gypsum, 3. selenite gypsum, 4. brecciated gypsum or gypsarenite, 5. porphyroblastic gypsum, 6. fine lenticular gypsum, 7. crystalloblastic or blocky anhydrite, 8. prismatic anhydrite, 9. epigenetic anhydrite, and 10. felty epigenetic anhydrite.

Gypsum: The alabastrine gypsum consists of small to large, commonly poorly defined interlocking crystals, many with irregular extinction. Anhydrite inclusions are very numerous around the gypsum crystals. They are very small and appear as irregular shreds with random orientation (Figure 9C). Satin spar gypsum (or fibrous alabastrine gypsums) are present at the boarder of the gypsum grains and in the gypsum veins, having a displacive (intrusion) relationship. Usually, they are a few micrometers or millimeters in thickness and consist of vertically arranged fibers.

Selenitic gypsum could be recognized at both macroscopic and microscopic scale. In the core it is found as large, elongated, saber-like gypsum crystals. Under the microscope it can be seen as large crystals floating in alabastrine and felty epigenetic anhydrite matrix showing peculiar fabric of the twin, perpendicular or sub-perpendicular to the bedding plane, surrounded by rupturally deformed secondary gypsum crystals (Figure 9D).

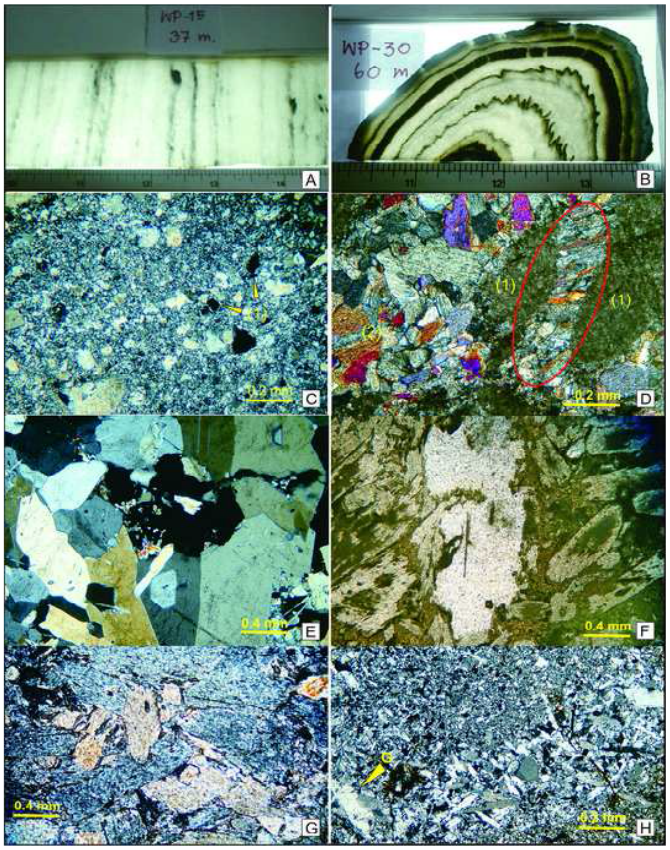

Figure 9: (A) Alabaster gypsum with thin lamination and carbonate clasts; (B) Alabaster gypsum with distorted laminated gypsum; (C) Photomicrograph of alabastrine gypsum displaying small to large crystals, poorly defined interlocking crystals with scattered pyrite crystals, (arrow 1), crossed Nicols; (D) Photomicrograph of satin spar gypsum (red circle) veins, in carbonate clast (1), crossed Nicols; (E) Photomicrograph of gypsarenite showing granitoid texture, angular grains and interlocking with no apparent cementing, crossed Nicols; (F) Photomicrograph of selenitic secondary gypsum showing limpid crystalline core surrounded by rupturally deformed secondary gypsum grains, crossed Nicols; (G) Porphyroblasts gypsum, some elongated crystals show replacement of felty epigenetic anhydrite, crossed Nicols; and (H) Gypsum porphyroblasts (G) in a fine lenticular gypsum texture with few dispersed anhydrite remains, crossed Nicols.

The gypsarenite is found associated with alabastrine gypsum and in the gypsum veins. Gypsarenite consists of grains of recrystalline gypsum. The texture of the gypsarenite is present as a granitoid rock, the grains are angular, monocrystalline, and interlocking with no apparent cementation (Figure 9E). The cementation of the rock is mostly made by direct contact between the gypsum individuals. In the gypsarenite, the lacks of inverse graded bedding (which is the primary texture of gypsum beds) and of textures, indicate transformations or replacements. Without any doubt the larger grains in this texture originated from selenitic secondary gypsum because this size is far above 0.5 mm, which is the dimension of the largest granules of primary gypsum, and also because they display twinning that was described as a typical feature for selenitic secondary gypsum (Figure 9F).

Porphyroblastic gypsum can be observed as large crystals (Figure 9G) under the microscope associated with alabastrine and lenticular gypsum (Figure 9H). Recently, it was found that lenticular gypsum can be formed in intertidal zones [23].

These gypsum textures, together with the deformation of the embedded sediments, the elongation of the crystal, and the crystalloblastic textures, clearly show that crystal neoformation took place with mechanical strains due to a volume increase. Hence, the petrography of gypsum infers that the gypsum is secondary gypsum which was transformed from the rehydration of anhydrite.

Anhydrite: The anhydrite occurs as a dense, white to grayish rock, laminae usually a few millimeters to centimeters thick, alternating with carbonate mud and clay laminae (Figure 10A). The anhydrite laminae are almost entirely made up of anhydrite grains separated by very thin carbonate layers, which have a micrite-microsparite texture, with partially dolomitized and scattered pyrite crystals. These carbonate laminae are lithologically comparable to the carbonate laminae intercalated with gypsum.

Microscopically, the anhydrite laminae consist of densely packed, elongated anhydrite laths with dimensions mostly less than 75 μm. Some crystals range up to 100 μm long. Overall, most of the anhydrite crystals show random orientation, a texture termed decussate or subfelted to felted [24,25]. Anhydrite could be recognized as crystalloblastic or blocky anhydrite, prismatic anhydrite, epigenetic anhydrite, and felty epigenetic anhydrite texture. The carbonate lamellae have a micrite-microsparite texture, with partial dolomitization, and contain detrital quartz and pyrite crystals.

Crystalloblastic or blocky anhydrite occurs as mosaics of commonly elongated, euhedral to subhedral anhydrite crystals with partially corroded margins (Figure 10B). Most of the crystals are blocky and have dimensions up to 50 μm in length. The fabric is felted and/or corrotopic, i.e., it consists of larger, partially corroded porphyroblastic crystals that float in a finer crystalline matrix. Some crystals show no

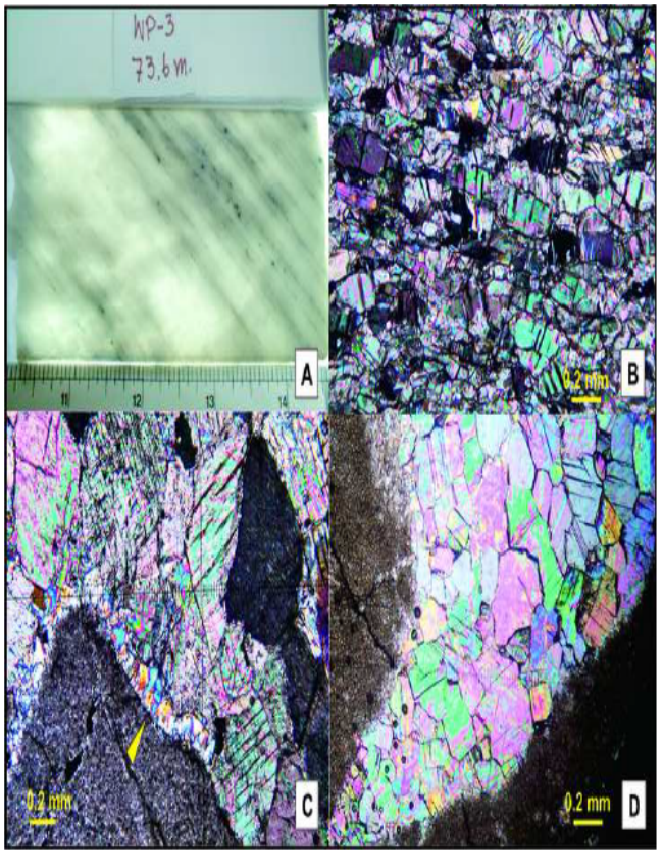

Figure 10: (A) Dense anhydrite with thin carbonate lamination; (B) Photomicrographs of crystalloblastic anhydrite showing elongated, parallel or nearly parallel crystals, crossed Nicols; (C) Photomicrograph of prismatic anhydrite developed at the carbonate clast rim (arrow), crossed Nicols; and (D) Photomicrograph of anhydrite porphyroblast vein showing blocky crystals of anhydrite, crossed Nicols.

regular shape, but some of them display a very distinct rectangular outline. This texture is formed when gypsum transforms to anhydrite. Prismatic anhydrite is found developed at the rim of the carbonate clasts (Figure 10C).

Epigenetic anhydrite is a secondary anhydrite which can be observed replacing the primary as well as secondary gypsum [26-28]. This secondary anhydrite is designated as epigenetic anhydrite [29]. Its texture forms as spindle-shaped and rhomboidal individuals characterized by an elongation, often oblique to cleavage and optical axis, and lack well defined cleavage. Some parts of the rock have an aligned-felted texture in which anhydrite laths show preferred orientation parallel or subparallel to the bedding. The elongation of the individuals of epigenetic anhydrite is very striking and probably resulted by rehydration.

The orientation of crystalloblastic anhydrite may have been caused by direct pressure or probably due to recrystallization flow. The porphyroblasts (Figure 10D) took place when the stress was removed, as is in this case where the rebound or growth phenomenon can be noted.

Anhydrite in LWS deposits has been recrystallized. This is indicated by the crystalloblastic texture of the anhydrite. The petrographic study of anhydrite yield that anhydrite also show secondary features, which could be transformed from the former gypsum by dehydration process. Therefore, the sulphate deposits here should originally be deposited as gypsum with carbonate and siliciclastic rocks. Then gypsum was subsequently transformed to anhydrite upon burial as a consequence of rising temperature and pressure, this process could have occurred during subsidence of the deposits. Anhydrite re-emerged to near surface due to tectonic movements probably associated with the uplift of the Loei Fold Belt, and the upper part was rehydrated back to gypsum.

Associated rocks

Carbonate rocks: Carbonate rocks are found present throughout the boreholes, lying above, interbedded or intercalated with other rocks, and underlying the gypsum-anhydrite at the end of the boreholes. The cores of carbonate rocks are always found broken and karstification could be recognized from some. The carbonate rocks found in the boreholes include carbonate mudstone, wackstone and packstone, algal boundstone, and fenestral carbonate mudstone. The thickness of each lithology varies from less than 1 m up to 40 m. The most common carbonate rocks found in the boreholes are carbonate mudstone and wackstone. The carbonate mudstone beds are found extensively in the boreholes of the exploration area. These beds are highly fractured with calcite veins filling, well laminated with bird's eye structure, found with minor thin shale beds intercalated, and consists of partially dolomitized and carbonaceous lime mudstone. Beds are light to dark grey in color and include detrital sand grains, unidentified microfossils, and fine-grained skeletal debris. Two sets of stylolites are present in these beds, one set is parallel to the bedding and the other set is perpendicular to the bedding plane. The wackstone is light to dark grey in color and commonly found alternated with carbonate mudstone and algal boundstone in the boreholes. The beds are difficult to recognize due to

the badly broken core samples. The rock shows matrix supported texture which contains abundant peloids and bioclasts of foraminifera, algal fragments, brachiopods fragments, crinoids and corals. Bioturbation, fracture filled with calcite, stromatolite structure, wavy stylolite and Fe-staining are common. Sedimentary structures found in this lithofacies are lamination, bird's eye structure, stylolite, fracture (most of the fractures have calcite filling), and bioturbation. Pyrite is also abundant in these carbonate beds with some other opaque minerals.

Theoretically, massive carbonate mudstone beds deposit in a shallow marine environment where carbonate particles accumulate in quiet water areas not affected by currents. However, thin and laminated carbonate mudstone beds accumulate in moderate energy areas where cyanobacterial mats bound the sediment surfaces [30]. For the carbonate mudstone in this area El Tabakh and UthaAroon suggested them to be accumulated in a subtidal environment. Normally, skeletal and peloidal wackstone and packstone lithofacies are deposited above storm-wave base and are typified by open marine fauna [31].

Siliciclastic rocks and volcanic rocks: The siliciclastic rocks, occasionally found in some boreholes are interbedded with carbonate rocks and gypsum. The beds are composed of intercalated sandstone and mudstone, some beds are sand dominant and some beds are mud dominant, but most of the siliciclastic rocks in the boreholes are mudstone. The sandstone beds are generally thinly even bedded, but in some boreholes, they are up to 15 m thick (WP2) and occasionally fractured and filled with calcite. The sandstone is fine- to medium-grained, white, light brown or light yellowish brown in color. The mineral constituents are composed mainly of quartz, minor opaque minerals, and varying contents of dolomite, calcite, and carbonaceous lime mudstone. These sandstone beds are alternated with siltstone and mudstone, finely to wavy laminated. Some beds contain mudstone intraclasts and load structure. Sandstone beds display lateral variation of depth profile. Mudstone beds (or mud dominant beds) are more common in the boreholes than sandstone. The color of these beds is greenish grey to dark gray. The beds are well-laminated with layers of coarser lithoclasts and show graded bedding at some intervals. Some beds show wavy lamination, bioturbation, and fluidization.

The thin, even bed with graded beds of sandstone and limestone within the mudrocks may represent storm deposits in an open marine shelf environment. Bioturbation is common. Mudrocks of the marine shelf are a major component of all shelf and epeiric-sea sequences in the geological record and they usually pass laterally (shorewards) or vertically into limestones or sandstones of the shallow-water near-shore zone [31].

Conglomerate beds are occasionally present in some boreholes. Breccia beds are always found in thick sandstone beds and near the karstification in carbonate beds. The conglomerate is found overlain and interbedded with fractured limestone as conglomeratic limestone. Carbonate clasts are up to 15 cm in size and are commonly matrix supported and locally mixed with detrital quartz grains. The beds are calcareous containing red colored sandy matrix (Figure 9). The inclined stylolite surfaces are present in these beds. Breccia beds are more common in this deposit. Most of the beds are brecciated limestone and semi-consolidated breccia intervals. The components of the breccia are limestone and sandstone with minor mudrocks.

Volcanic rocks are present in the east of the deposits. These are dominantly andesite, rhyolite, and dacite, which have been assigned to the Permo-Triassic age. The drilled cores show that small andesitic and rhyolitic rocks cross cut the gypsum layers in many boreholes such as WP2, WP11, WP15, and WP29. The relationship between the gypsum and volcanic dikes indicates that the gypsum is definitely older than Permo-Triassic.

Discussion

Combination of facies and petrographic characteristics reveal that the foregoing described evaporites show features supporting both primary and secondary formations. In addition, the petrographic study also show that a great part of the secondary gypsum might have been formed under the influence of a near surface deposition, thus reflecting the original brine characteristics. In addition, the thin layers of carbonate and shale in the gypsum-anhydrite deposits show typical horizontal bedding planes.

This gypsum morphology is similar to satin spar gypsum commonly recorded as fracture fillings in many publications [32-36,8]. After replacement took place, the beds were slightly deformed, but kept the primary horizontal bedding. Although clear evidence is lacking, the absence of other types of secondary gypsum in the light gypsum beds suggests that such replacement took place shortly after deposition, nevertheless, still under the strong influence of the primary brine. Therefore, despite their authigenic nature, the satin spar gypsum is considered as a reflex of the primary evaporite bedding.

Despite the many varieties of evaporites recorded in the LWS area are presented underground near Loei river, these deposits display many petrographic and faciological attributes that are consistent with an early to late stage of a gypsum-anhydrite formation. These types of evaporites prevail particularly in the area, where laminated gypsum facies dominate. In this area, burial phases of gypsum seem to have developed only where gypsum was remobilized during halokinesis [37-45].

The lack of significant deep diagenetic modification such as nodular anhydrite of the Wang Saphung evaporate is recorded also by studies focusing on the limestones and shales interbedded with the evaporites. The limestones are dominated by calcimudstone, peloidal wackstone or packstone, algal boundstone, and fenestral carbonate mudstone with only local evidences of cementation or replacement. These beds suggest a shallow marine deposition, being accumulated in a tidal flat to subtidal environment. The beds display extensive karstification and cavity fill. The siliciclastic and conglomerate and breccia beds are also present in the sequences of the deposits. The sandstone beds indicate a marine shelf environment while the conglomerate and breccia indicate a basin-margin slope deposit developed by over-steepening and subsequence collapse of the platform. However, the conglomerate and breccia in this deposit suggest being formed from a collapse or tectonics [46-50].

Conclusion

The results from detailed lithologic and petrographic studies yield that these sulfate deposits have passed through at least 4 stages of diagenetic alterations, these are;

(1) Precipitation of bedded gypsum in a hypersaline basin. It is suggested that a large portion of the evaporite was originally precipitated as bedded gypsum in a restricted hypersaline basin. This is indicated by the laminated texture of the sulfate beds and the prominent laminae of carbonate in gypsum and anhydrite which are primary sedimentary textures of stratiform sedimentary deposits. Additionally, there is no evidence of nodular anhydrite grains which is a typical form of anhydrite formed at Earth's surface (i.e., subkha environment).

(2) Gypsum-to-anhydrite transformation resulting from burial diagenesis. These alterations are indicated by the corrotopic and felted epigenetic anhydrite which form when gypsum transforms to anhydrite.

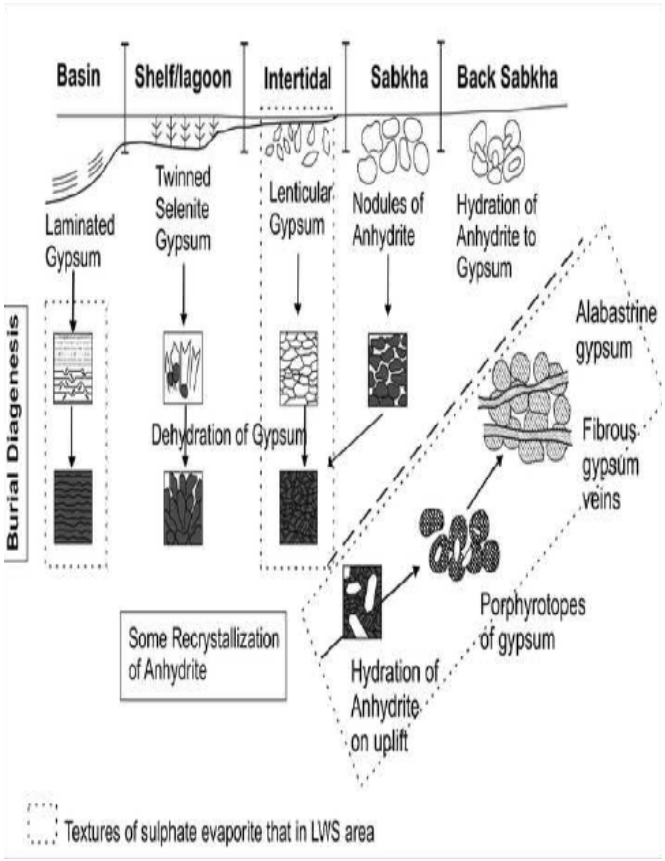

Figure 11: Schematic illustration of the gypsum-anhydrite cycle showing mineralogical and textural changes, from the surface, into the subsurface, and on uplift in various environment of depositions, in the is the texture that we can observe in LWS sulphate deposits (modified after Warren in 1999 and Warren again in 2006).

(3) Rehydration of anhydrite-to-gypsum. This is indicated by the distortion of gypsum rocks, which result from the increase of volume due to rehydration of anhydrite to gypsum and recrystallization of anhydrite and/or primary gypsum to secondary gypsum (alabastrine, selenitic, and gypsarenite secondary gypsum).

(4) Uplift and erosion during re-expose of gypsum. This is indicated by karstification and dissolution of cavities in the sulfate bodies, the presence of gypsarenite without felty anhydrite replacement, and gypsarenite veins which are the latest veins cutting through the sulfated unit. These secondary gypsarenite indicate a later stage rehydration which is a result of transformation from secondary selenitic gypsum [51-66].

From the schematic diagram of depositional environment and alteration of evaporite/sulphate shown in Figure 11, we found the textures in the rectangular dash line in LWS sulphate deposits. Hence, the lithologies of our sulphate deposits could be interpreted as sub-aqueous precipitation in a basin, probably shallow-lagoon setting or restricted marine, and may be accompanied with an intertidal deposition.

Timing of the deposition is suggested to be during Late Carboniferous. This is indicated by the cross cut of Permo-Triassic volcanic dikes (age of this volcanic dikes are equivalent to the study by Intasopa and Khin Zaw in gypsum and the associated carbonate beds that are dated (by microfossils) to be below a Late Moscovian (Podolskian–Myachkovskian) in Late Carboniferous [17,18,21]. The environment and the age of the deposits in this paper is only a suggestion based on the study of core logging of the exploration wells in the area and petrography of selected samples, and interpretation of previous works on the gypsum deposits in this area. Therefore, it is necessary to verify the results by further studies such as a geochemical study of the deposits as well as a detailed analysis on the geologic controls and tectonic setting of the adjacent areas governing their transformation. These studies would add to the understanding of the depositional setting and diagenetic history as well as the origin of the deposits.

Acknowledgements

The author would like to acknowledge Department of Primary Industries and Mines, Thailand, who provided the data for this research. The author also shows appreciation to the Department of Geology, Chulalongkorn University for providing excellent cooperation and laboratory support during this research.

References

1. Warren JK (1989) Evaporite sedimentology: Its importance in hydrocarbon accumulation. Prentice Hall, Eaglewood Cliffs, NJ pp: 285.
2. USGS (2010) Mineral commodity summaries, United States Government Printing Office, Washington.
3. USGS (2012) Mineral commodity summaries, United States Government Printing Office, Washington.
4. Department of Mineral Resources (DMR) of Thailand (1977) Gypsum-economic geology bulletin no.17: Economic Geology Division, DMR, Thailand.
5. Utha-Aroon C, Surinkum A (1995) Gypsum exploration in Wang Saphung, Loei: In: Proceeding of the International Conference on Geology, Geotechnology and Mineral Resources of Indo-China, Khon Kaen University, Khon Kaen, Thailand pp: 257-266.

6. Kuttikul P, Surinkum A, Utha-Aroon C (1997) Application of gravity survey in gypsum exploration. Wang Saphung, Loei. Pp: 1-37.
7. Pisutha-Arnond V, Kusakabe M, Khantaprab C, Vedchakanchana S (1997) Sulfur and oxygen isotope study of the Pichit - Nakorn Sawan gypsum/anhydrite deposit: An implication on the age of its formation. pp: 188-199.
8. El Tabakh M, Utha-Aroon C (1998) Evolution of Permian carbonate platform to siliciclastic basin: Indo-China Plate, Thailand. Sedimentary Geol 121: 97-119.
9. Cooper MA, Herberrt R, Hill GS (1989) The structural evolution of Triassic intermontane basins in Northeastern Thailand. pp: 231-242
10. Mitchell AHG (1986) Mesozoic and Cenozoic regional tectonics and metallogenesis in mainland SE Asia. GEOSEA V 20: 221-239.
11. Metcalfe I (1988) Origin and assembly of south-east Asian continental terranes. 37: 101-118.
12. Bunopas S (1981) Palaeogeographic history of western Thailand and adjacent parts of southeast Asia – a plate tectonics interpretation.
13. Hutchison CS (1998) Geological evolution of South-East Asia.
14. Barr SM, Macdonald AS (1991) Toward a late Paleozoic–early Mesozoic tectonic model for Thailand. Thailand J Geosci 1: 11-22.
15. Chonglakmani C (1984) Geological map of Udon-Thani-Wang Wiang Quadrangle. Scale 1: 25,000 DMR Bangkok, Thailand.
16. Chairangsri C, Hinze C, Machareonsap S, Nakornsri N, Silpalit M, et al. (1990) Geological map of Thailand 1: 50,000 Exploration for sheet Amphoe Pak Chom 5345 I, Ban Na Kho 5344 I, Ban Huai Khob 5445 IV and King Amphoe Nam Somm 5444 V, Geol. Ib. B73, Hanover. pp: 109.
17. Intasopa SB (1993) Petrology and geochemistry of the volcanic rocks of the central Thailand Volcanic Belt, (Unpublished manuscript).
18. Kamvong T, Khin Z (2009) The origin and evolution of skarn-forming fluids from the Phu Lon deposit, northern Loei fold belt, Thailand: Evidence from fluid inclusion and sulphur isotope studies. J Asian Earth Sci 34: 624-633.
19. Department of Mineral Resources (DMR) of Thailand (2007) Geological Map of Loei Province, Department of Mineral Resources, Bangkok, Thailand.
20. Surakotra N, Pisutha-Arnond V, Warren JK (2005) Some characteristics of gypsum-anhydrite deposit in the Loei-Wang Saphung, Northeastern Thailand.
21. Fontaine H, Salyapongse S, Utha-Aroon C, Vachard D (1997) Age of limestones associated with gypsum deposits in northeast and central Thailand: A first report, CCOP Newsletter. 21: 6-10.
22. Khin Z, Meffre S, Kamvong T, Khositanont S, Stein H, et al. (2009) Proceedings of the Tenth Biennial SGA Meeting, Townsville, August, 2009, Townsville, Australia.
23. Warren JK (2006) Evaporites: Sediments, resources and hydrocarbons. p: 1035.
24. Shearman DJ, Fuller JGCM (1969) Anhydrite diagenesis, calcitization and organic laminites. Winnipegosis Middle Devonian, Saskatchewan. Bull Ca Petrol Geol 17: 496-525.
25. Maiklem WR, Bebolt DG, Glaister RP (1969) Classification of anhydrite – A practical approach. Can Pet Geol Bull 17: 194-233.
26. Brown LS (1931) Cap-rock petrography: American Association of Petroleum Geology Bulletin 15: 509-529.
27. Von-Gaertner HR (1932) Petrographie und paläogeographische stellung der gipse vom südrande des harzes. Jb Preuss geol 53: 655-694.
28. Goldman MI (1952) Deformation, metamorphism, and mineralization in gypsum-anhydrite cap rock sulphur salt dome, Louisiana. Geolo Soci America Memoir 50: 169.
29. Ogniben L (1957) Petrografia della serie solfifera siciliana econsiderazioni geologiche relative. Mem Descr Carta Geol Ital XXXIII 1-275.
30. Jones B, Desrochers P (1992) Shallow platform carbonates. geological association of Canada, Toronto. pp: 277-301
31. Tucker ME (1992) Sedimentary petrography: An introduction to the origin of sedimentary rocks, (2ndedn), Blackwell Scientific Publications, Oxford, London. pp: 260.
32. Richardson WA (1920) The fibrous gypsum of Nottinghamshire. Min Mag 91: 77-95.
33. Shearman DJ, Mossop G, Dunsmore H, Martin M (1972) Origin of gypsum veins by hydraulic fracture. Trans Inst Min Metall 81B: 149-155.
34. Mossop GD, Shearman DJ (1973) Origin of secondary gypsum rocks. Trans Inst Min Metall B82:147-154.
35. Stewart AJ (1979) A barred-basin marine evaporite in the upper proterozoic of the amadeus basin, central Australia. Sedimentology 26: 33-62.
36. Gasiewicz A, Czapowski G, Kasprzyk A (1998) Gypsum-to-anhydrite transition in the miocene of southern poland. J Sedimentary Research 68: 223-234.
37. Aref M (2003) Lithofacies characteristics, depositional environment and karstification of the late miocene (Messinian) gypsum deposits in the northern western desert. Egypt Sedimentology of Egypt 11: 9-27.
38. Barr SM, Charusiri P (2011) Volcanic rocks in Thailand. Geological Society, London. pp: 415-440.
39. Bunopas S, Vella P (1978) Late Palaeozoic and Mesozoic structural evolution of Northern Thailand. Bangkok. pp: 133-140.
40. Bunopas S (1983) Paleozoic succession in Thailand. Geological Society of Thailand Bangkok Thailand. pp: 39-70.
41. Burrett CE, Carey SP, Wongwanich T (1986) A Siluro-Devonian carbonate sequence in northern Thailand. J Southeast Asian Earth Science 4:215-220.
42. Burrett CE, Long J, Stait B (1990) Early to Middle Paleozoic biogeography of Silurian and Devonian in the Yunnan-Malaya Geosyncline. Paleontological Society of Japan Transactions and Proceedings. 65: 24-46.
43. Charusiri P, Suwannachote P, Nutchanong T, Saengsila S, Yaemniyom S (1995) Alteration and Pb-Zn (Au) mineralization of the Phu Chang area, Changwat Loei, NE Thailand: Implications for a proposed genetic model. pp: 201-203.
44. Charusiri P, Daorek V, Archibald D, Hisada K, Ampaiwan T (2002) Geotectonic evolution of Thailand A new synthesis. J Geological Society of Thailand 1: 1-20.
45. Dunham RJ (1962) Classification of carbonate rocks according to depositional texture. American Association of Petroleum Geologists. pp:108-121.
46. Ferrarase F, Macaluso T, Madonia GPA, Sauro U (2002) Solution and recrystallization processes and associated landforms in gypsum outcrop of Sicily: Geomorphology 49:25-453
47. Fontaine H, Salyapongse S, Tian P, Vachard D (2005) Chapter III: An overview of the Carboniferous of Thailand with new data on the Carboniferous of northeast and northwest Thailand.
48. Gustavson TC, Hovorka S, Dutton AR (1994) Origin of satin spar veins in evaporite basins. J Sed Res A 64: 88-94.
49. Hardie LA (1967) The gypsum-anhydrite equilibrium at one atmosphere pressure. American Mineralogy 52:171-200.
50. Intasopa S, Dunn T (1994) Petrology and Sr-Nd isotopic systems of the basalts and rhyolites Loei Thailand. J Southeast Asian Earth Sciences 9: 167-180.
51. Jacobson HS, Pierson CT (1969) Mineral investigations in Northeastern Thailand. United States Geological Survey Professional Paper.
52. Kasprzyk A (1995) Gypsum-to-anhydrite transition in the Miocene of southern Poland. J Sedimentary Research A65: 348-357.
53. Zaw K, Kamvong T, Khositanont S, Mernagh TP (2011) Oxidized vs. reduced Cu-Au Skarn formation and implication for exploration, Loei and Troung Son Fold Belts, SE Asia, Proceedings of International Conference on Geology, Geotechnology and Mineral Resources of Indo-China (GEOINDO 2011), Khon Kaen, Thailand.
54. Khositanont S, Zaw K, Ounchanum P (2009) Mineralisation characteristics and ore fluid of Huai Kham on gold deposit northern Thailand. Advances in Geosciences (AOGS) 13:1–12.
55. Laveine JP, Ratanasthien B, Sithirach S (1993) The carboniferous flora of Northeastern Thailand: Its paleogeographic importance. Comptes Rendus de l'Académie des Sciences de Paris 317: 279-285.
56. Laveine JP, Ratanasthien B, Sithirach S (1994) The Carboniferous flora of Na Duang Coal Mines, North-eastern Thailand, Its paleogeographic interest.
57. Laveine JP, Ratanasthien B, Sititach S (2003) The carboniferous flora of northeastern Thailand. Revue Palaeobiologique Geneve 22: 761-797.

58. Laveine JP, Vachard D, Ratanasthien B, Sithirach S (2003b) The lower carboniferous Na Duang marine band (Na Duang Coal Mine, Loei District, Northeastern Thailand). Revue de Paléobiologie Genève 22: 799-809.

59. Laveine JP, Ratanasthien B, Sititach S (2009) The carboniferous flora of northeastern Thailand: Additional documentation from the Na Duang-Na Klang basin. Revue de Paléobiologie, Genève 28: 315-331.

60. Metcalfe I (2002) Permian tectonic framework and palaeogeography of SE Asia. J Asian Earth Sciences 20: 551-566.

61. Neusuparb K, Charusiri P, Meyers J (2004) New processing of airborne magnetic and electromagnetic data and interpretation for subsurface structures in the Loei Area. Northeastern Thailand Science Asia 31: 283-298.

62. Rattanasthien B (2011) Coal deposits, Geological Society, London.

63. Sando WJ (1995) Geologic history of salt beds and related strata in the upper part of Madison group (Mississippian) Williston basin, Montana and North Dakota. US Geological Survey Bulletin.

64. Sengor AMC (1985) East Asian Tectonic collage. Nature 318: 1-17.

65. Utha-Aroon C, Paiyarom A, Neowsupap C, Anukul S (1995) Application of electro-magnetic (EM) survey in gypsum exploration, Wang Saphung, Loei, Mineral Resources Development Division Report.

66. Ueno M, Chareonthitirat T (2011) Carboniferous and Permian, Geological Society, London. pp: 71-136.